Sponges architecture by colour: new insights into the fibres morphogenesis, skeletal spatial layout and morpho-anatomical traits of a marine horny sponge species (Porifera)

G. A. Stocchino, T. Cubeddu, R. Pronzato, M. A. Sanna & R. Manconi

Published online: 03 Mar 2021.

Submit your article to this journal ⤤

Article views: 206

View related articles ⤤

View Crossmark data ⤤

Taylor & Francis
Taylor & Francis Group

Check for updates

Sponges architecture by colour: new insights into the fibres morphogenesis, skeletal spatial layout and morpho-anatomical traits of a marine horny sponge species (Porifera)

G. A. STOCCHINO [1,*,**], T. CUBEDDU [1,**], R. PRONZATO [2], M. A. SANNA [1], & R. MANCONI [1]

[1]*Dipartimento di Medicina Veterinaria, Università di Sassari, Sassari, Italy, and* [2]*Dipartimento di Scienze della Terra, dell'Ambiente e della Vita, Università di Genova, Genova, Italy*

Abstract

This paper focuses on the skeletal architecture and morphotraits of the Mediterranean horny sponge *Sarcotragus spinosulus* (Demospongiae, Keratosa, Dictyoceratida, Irciniidae). This special endoskeletal system consists of a dense, variably complex connective architecture, which extends throughout the entire sponge body and is embedded in an abundant jelly-like extracellular matrix (ECM). To investigate the topographic arrangement and micro-morphotraits of these connective structures in detail and by colour, also during morphogenetic processes, histology techniques using light microscopy are essential. New information is provided on the coordinated morphogenetic processes that characterize the growth and assembly of collagenic prototype structures in the matrix of fibrous skeletal elements and drive skeleton remodelling. Our results also highlight some novelties and some remarkable peculiarities of fibrous, filamentous and fibrillar components at the levels of both composition and structure. The morphofunctional significance of skeletal architecture is suggested in the background of the anatomical complexity of *S. spinosulus*.

Keywords: *Connective architecture, fibrous/filamentous/fibrillar structures, morphogenesis, histology,* Sarcotragus spinosulus

Introduction

In Demospongiae Sollas, 1885, the exclusively organic filamentous and reticular fibrous skeleton represents a key evolutionary novelty in the phylogeny of Keratosa Grant, 1861 (Demospongiae widespread in shallow and deep water in all oceans) of the clade Dictyoceratida Minchin, 1900, known classically as horny sponges or also as tricky tree sponges *sensu* Erpenbeck et al. (2020). The spatial layout and abundance of filaments, coexisting with the irregular reticulum of anastomosing fibres, is typical of the monophyletic family Irciniidae (Cook & Bergquist 2002; Pronzato & Manconi 2011; Erpenbeck et al. 2020). These predominantly collagen structures play a key role in the skeletal architecture of the Irciniidae Gray, 1867 family and are suggestive of their divergent evolutionary trends (Garrone 1985; Hooper & van Soest 2002; Erpenbeck et al. 2020).

The development of electron microscopy techniques has meant that sponge studies performed by means of light microscopy have been neglected, even though morpho-anatomic traits can be discerned in detail at this latter level of investigation. Although histological and histochemical analyses in the 1950s-70s revealed an outstanding range of structural architectures of sponges (Gross et al. 1956; Cowden 1970; Brien et al. 1973; Garrone et al. 1973; Cowden & Harrison 1976; Garrone 1978, 1985), there are still knowledge gaps in this field. Bergquist et al. (1998) highlighted the performances of the histological analyses as a key tool to understand the architecture and composition of the horny sponges skeleton.

The aim of the present study was to extend basic knowledge of the skeletal architecture, spatial arrangement and topographic distribution of collagen structures (fibres, filaments and fibrils) to also

support applied research on biomaterials of sponges. Our experimental model species is *Sarcotragus spinosu* Schmidt, 1862, the type species of the genus *Sarcotragus* Schmidt, 1862 (Demospongiae, Keratosa, Dictyoceratida, Irciniidae). Here, we provide a morpho-anatomical histological analysis of the skeletal pattern of this species and its morphogenetic processes of fibres growth and remodelling.

Methods

Experimental design, study area and sampling

Our morpho-anatomical targets were to (a) verify the identity at the species level of samples from *in situ* farmed clones, and (b) characterize skeletal microstructures by means of differential staining, confocal microscopy and Scanning Electron Microscopy (SEM).

Clones of *Sarcotragus spinosulus* had been obtained during previous farming experiments on donors from the wild population inhabiting shallow water (0.2–3 m) rocky substrata, intermattes and rhizomes of *Posidonia oceanica* (L.) Delile, 1813 meadows in Porto Conte Bay (Figure 1, Sardinia, Italy) (see Perez-Lopez et al. 2017; Padiglia et al. 2018; Manconi et al. 2020; Manconi et al. 2020). This is a pristine area in the Capo Caccia - Isola Piana Marine Protected Area (MPA) in the Northern Sardinian Sea (Western Mediterranean).

Mariculture plant is located on special submerged man-made structures in a small marina in Tramariglio Cove (40°35′32.47″N, 8°10′11.50″E); plant modules are anchored to the underwater structure of a pier in shallow water (2–3 m depth), and are partially shaded by the pier (see Perez-Lopez et al. 2017; Padiglia et al. 2018). The cove is sheltered from the north-western wind, but exposed to the east wind and strong gales from the southwest.

Representative fragments of 3 clonal *S. spinosulus* (n = 12) were collected during cold and warm seasons (2018–2020) by means of a scalpel. Live sponges were photographed in the field (EOS G10, Canon, Japan). To investigate their morphological and histological traits, samples were kept in sea water in refrigerated bags, and transferred to the Zoology Lab, Veterinary Medicine Department, Sassari University, for microscopy analyses.

Diagnostic traits and morpho-anatomical analyses

A few hours (2–4) after collection, unstained samples of the sponges were examined in reflected and transmitted light with a low-magnification stereomicroscope.

For taxonomic analyses in the lab, samples were washed, dried at room temperature, labelled, registered in reference collections (KER-Sassari University, Zoology Lab, Veterinary Medicine Department) and processed. The diagnostic morphotraits considered for identification at the species level were as follows: growth form; dermal membrane (surface unarmed vs. armed with foreign material); conules and oscules (morphometry, shape and topographic distribution); general skeletal architecture; fine texture of fibrous network; primary, secondary and tertiary spongin fibres (topographic distribution and morphometry); collagen filaments (distribution, abundance and morphometry); ornamentation of fibres; and presence of foreign material in the pith of fibres. Thin slices of skeletons were obtained by dissecting samples by hand with scalpels under a Leica Wild M3C stereo-microscope; the slices
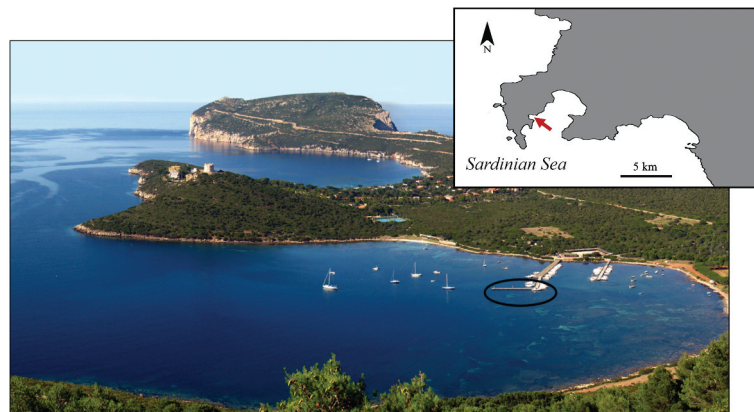

Figure 1. Study area in the Sardinian Sea (North-West Sardinia Island, Western Mediterranean Sea). Samples of a clonal strain of *Sarcotragus spinosulus* were taken in an experimental farming plant under a pier in a marina (circled in black) in Tramariglio Cove (red arrow) (inset indicates Porto Conte Bay, MPA Capo Caccia - Isola Piana).

were then macerated in sea water for a variable time according to the sample size and skeletal texture. After final rinsing and drying in ethanol, skeleton fragments were laid on a slide, under a weight, to be gently plated as flat thin slices; finally, the sections were cleared in Bio Clear (Bio-Optica, Milan) and mounted in Eukitt® under a coverslip. Observations were made by Light Microscopy (LM, Nikon ECLIPSE 80i, Japan) and photographs were taken with a Nikon Digital-Sight DS-FI camera (Japan). To characterize diagnostic micro-traits in detail, similar skeletal preparations for scanning electron microscopy (SEM Tescan Vega3, Czech Republic) were glued to a stub and sputter-coated with gold.

To characterize skeletal microstructures, several fragments were fixed at room temperature for 48 h in Bouin's fluid, dehydrated in an ascending ethanol series, cleared in xylene, and embedded in paraffin. Sections were cut at intervals of 4–5 μm and routinely stained with Masson trichrome and Azan-Mallory trichrome to evaluate the presence and distribution of collagen structures, and with Alcian blue stain (pH 2.5) to verify the presence of glycosaminoglycan (GAG)-like molecules. Slides were examined under a Nikon ECLIPSE 80i (Japan) light microscope and photographs were taken with a Nikon Digital-Sight DS-FI camera (Japan).

To obtain details of the collagen network of filaments, other sponge fragments were washed in PBS 1x and in mQ water, frozen at −80°C and then sectioned at 50–100 μm by means of a Leica CM1950 cryostat (medium Killik, Bio-Optica, Milan). Slides were observed and images were acquired by means of a Leica TCS SP 5 confocal microscope (Leica Microsystems, Germany) and processed by means of LAS AF Lite application software developed by Leica Microsystems CMS GmbH for contrast and brightness adjustment.

Abbreviations used in the figures

am: amorphous material; bg: bark (skeletal fibre cortex) growing; ca: canal; ch: choanosome; cp: cribrose plate; ec: ectosome; em: endobiotic microrganisms; ex: exopinacocyte; f: fibre; fc: fibrillar collagen; fi: filaments; hl: hyaline layer; pf: primary fibre; sn: subdermal network.

Results

General morpho-anatomy

The samples of *Sarcotragus spinosulus* displayed a massive, rounded growth form with variable body size. The surface was brownish in colour, black to dark grey *in vivo*; the interior was orange to light brown (Figure 2(A-B)). The body was slightly compressible, tough, and relatively difficult to cut or tear. The body surface was irregularly conulose and entirely covered by a dermal membrane consisting of a smooth, very thin hyaline layer (unarmed by detritus, Figure 2(A)) overlying a pigmented cellular layer of T-shaped exopinacocytes (Figure 3(D)). Conules had pointed apices, 1–2 mm in height and 1–5 mm apart, and an axis made by tips primary of fibres; conules were usually covered by a dermal membrane, sometimes fibre tips protruded from their apices (Figures 2(A), 3(A-C)). Oscules (up to 1 cm in diameter) were variably abundant, irregularly scattered, and had a small laminar collar (Figure 2(A-B)).

The three-dimensional endoskeleton was extended and embedded in the amorphous jelly-like Extracellular Matrix (ECM) of the entire ectosomal and choanosomal regions of the sponge body (Figure 2(C-D)).

Fibrous skeleton

The skeleton, orange to light brown in colour (*in vivo*), was made up of a fibrous, reticulate, anisotropic network with irregularly polygonal meshes of main cylindrical fibres (primaries) intersecting with irregularly transverse cylindrical fibres (secondaries) (Figures 4–5). This network also displayed laminar cribrose plates, which anastomosed the neighbouring main fibres to form quite rare fasciculate fibres (Figures 4–5). Main fibres (primaries), fascicular along large tracts, were ascending, radial, more or less parallel, and stout. Secondary fibres were thinner and irregularly scattered. Cribrose plates were frequently large and irregularly scattered in the network (Figures 4–5). Primaries fibres were morphologically heterogeneous along their length, with smooth linear tracts irregularly alternating with thicker nodulous tracts and laminar tracts (Figures 4–5). These tracts are distinguishable on the basis of their structure, composition and maturation phase.

Secondary fibres were entirely smooth and linear and irregularly arise both from primaries and from cribrose plates (Figure 5). Other, less frequent, partially "free" long fibres (secondaries) were also seen (Figure 5). Secondary fibres showed the same structural composition as the linear tracts of primaries. The diameter of secondaries and linear tracts of primaries (rounded sections) ranged 44-160 μm. The cribrose plates joining the primary fibres in fascicles displayed scattered meshes of variable number, shape and size (Figures 4(C, E), 5). All fibrous structures were made up of a bark surrounding a non-laminated axial pith (Figure 6). Moreover,
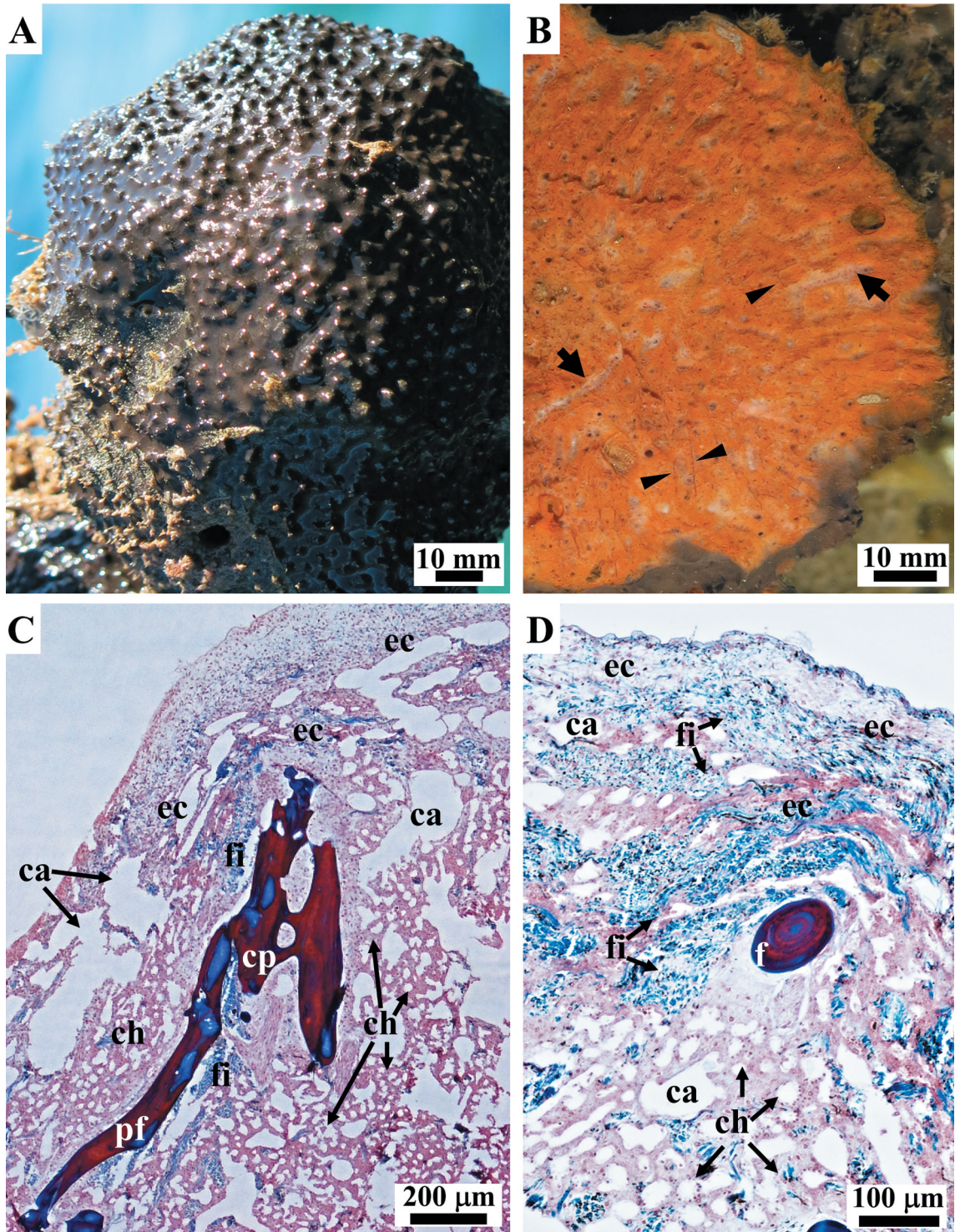
Figure 2. *Sarcotragus spinosulus*. Photo-macrographs *in vivo* and -micrographs of histological sections. (A). Habitus of a globular massive sponge with brownish surface, conules and a few oscules. (B). Body architecture (inner view, cross-section) with spiny brownish surface covered with conules, a dense, orange extracellular matrix with scattered whitish aquiferous canals (arrows) and orange-brownish ascending, more or less radial, primary skeletal fibres (arrowheads). (C-D). General views of ectosomal (ec, outer) and choanosomal regions (ch, inner) with evident canals (ca), primary fibres (pf), cribrose plate (cp), filaments (fi). (C-D LM, Masson trichrome).
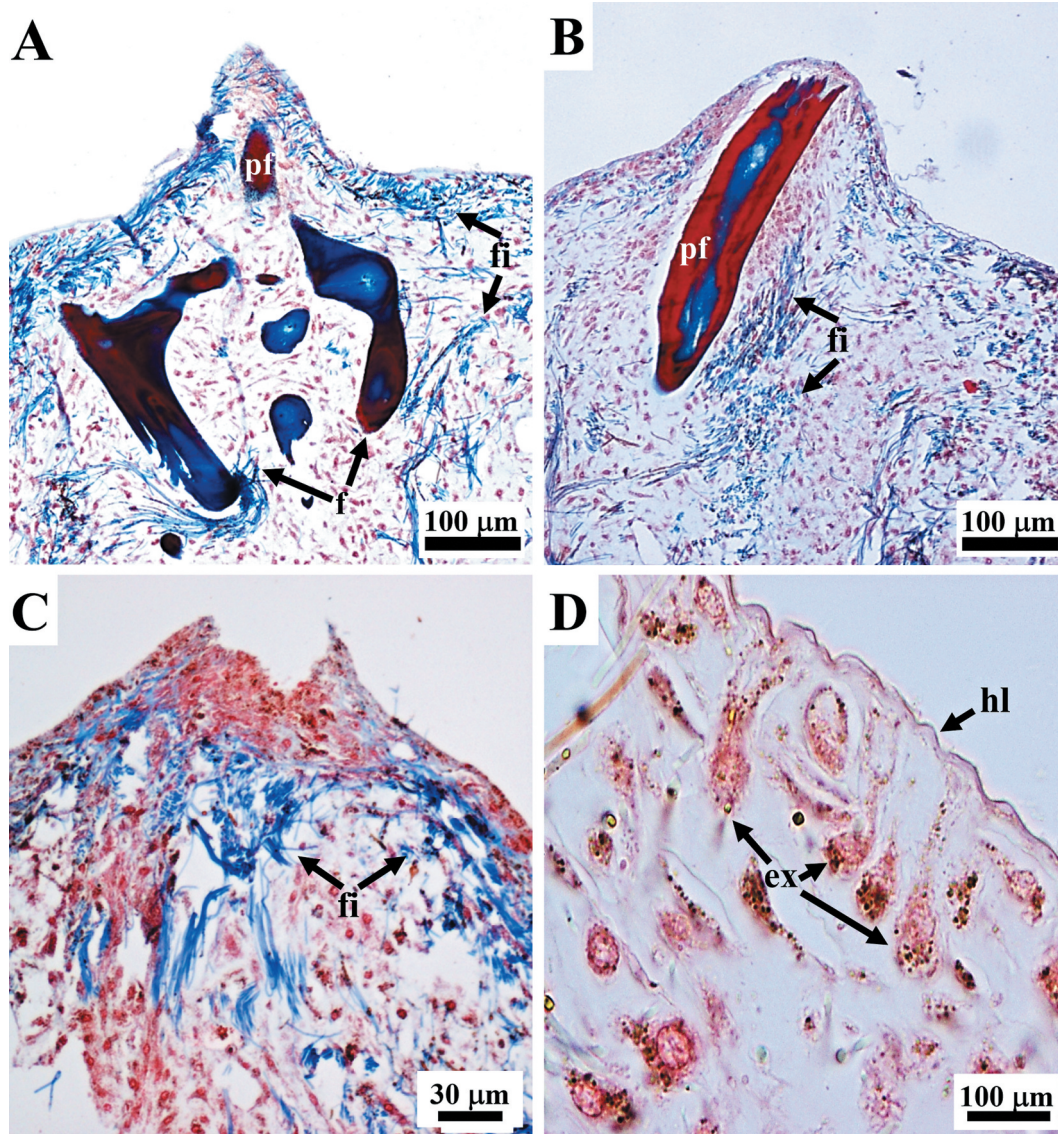
Figure 3. *Sarcotragus spinosulus*. LM photo-micrographs of histological sections. (A-C). Conules supported by apices of ascending primary fibres (pf in A and B) and a variably oriented network of bundles of filaments (fi) structuring the conular area (apex of conular fibre absent in C). (D). Outer hyaline layer (hl) overlying a pigmented cellular layer of T-shaped exopinacocytes (ex). (Masson trichrome).

proto-fibres originating *ex novo* were observed at different stages of formation and maturation.

Linear tracts of primary tracts. The bark was seen to be made up of dense concentric tightly adherent laminae (red with Masson trichrome, colourless with Alcian blue) alternating with layers of amorphous matrix (blue with Masson trichrome, colourless with Alcian blue) (Figure 6). On staining with Azan-Mallory trichrome, the bark appeared blue. Concentric layers appeared as growth lines. The non-laminated axial pith was amorphous (except when foreign spicules were present, i.e. intermittent core, see Figure 4) as was the matrix (blue) between the red layers of bark. On moving from the periphery to the inner part, the pith appeared blue to light blue to colourless on staining with Masson and Azan-Mallory trichrome (Azan-Mallory not shown). By contrast, Alcian blue tinged the inner pith light blue-turquoise (Figure 6(C-D)).

The ECM was also intensively coloured with Alcian blue (Figure 6(D)). Fibres sometimes showed signs of degeneration of the red layers, i.e. irregular scalloped margins (cross and tangential
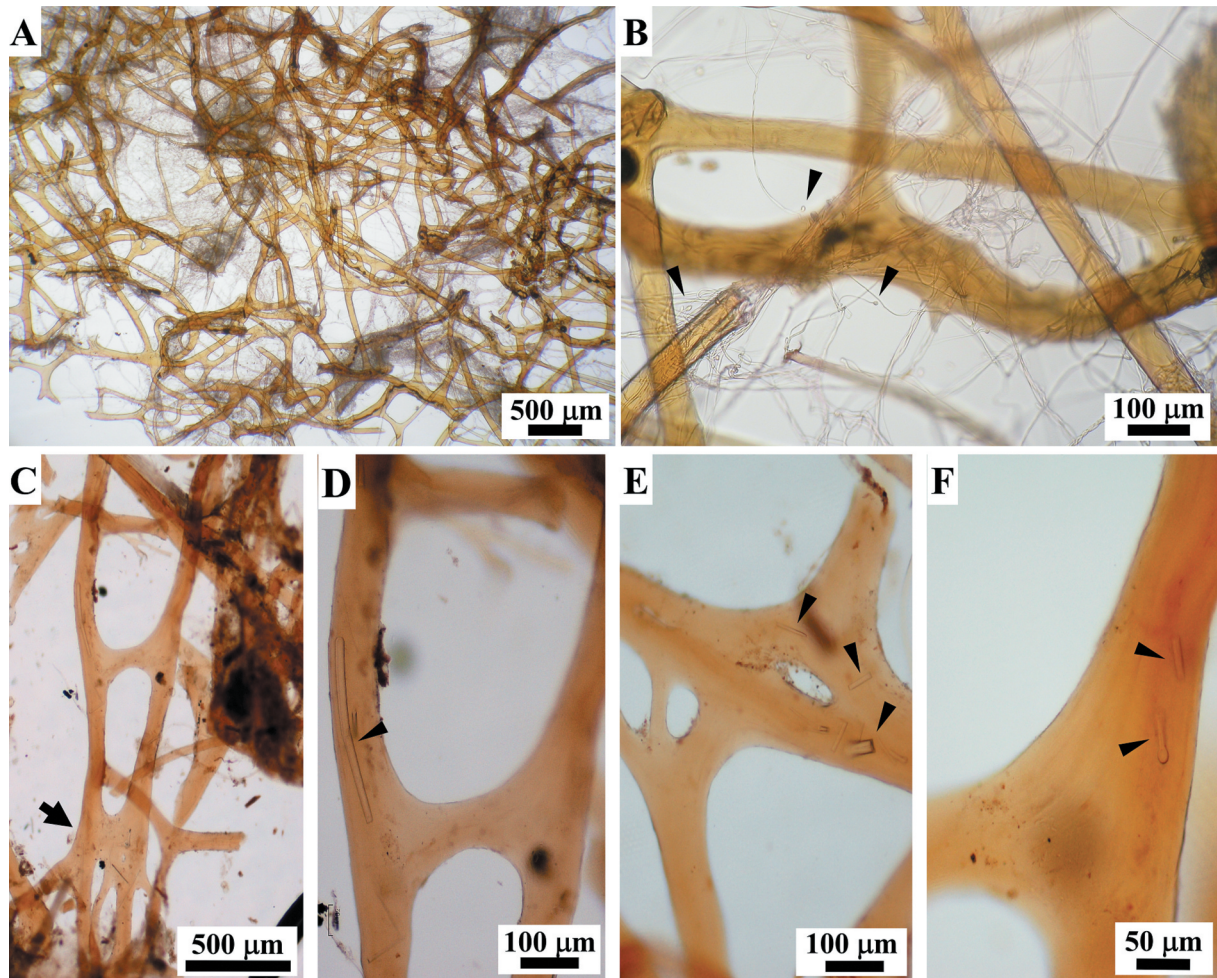
Figure 4. *Sarcotragus spinosulus.* LM photo-micrographs of the skeleton. (A). General view of fibrous and filamentous dissociated skeletal network with main ascending primary fibres, more or less radial, joining at nodes with thinner secondary fibres and cribrose plates (see Figure 5). (B). Irregular reticulate anisotropic fibrous network and dissociated thick- and thin-knob filaments (detail of a); arrowheads indicate knobs.(C). Primaries with cribrose plate as joining node (bottom) (arrow) bearing several secondaries. (D-F). Joining nodes and secondaries (detail of C). (E). Cribrose plate. (D-F). A few siliceous monaxial spicules (indicated by arrowheads) embedded in the axis of the fibre.

sections) alternating with layers of amorphous matrix (blue) (Figure 6(E-F)).

Laminar tracts of primary fibres. These tracts were seen to be composed of cribrose plates with irregular outlines (Figures 7(A-B)) made up of concentric tightly adherent laminae (red with Masson trichrome, colourless with Alcian blue) alternating with layers of amorphous matrix (blue with Masson trichrome, colourless with Alcian blue). On staining with Azan-Mallory trichrome, the bark appeared blue (not shown). On section, these plates (140–680 μm in diameter) had highly variable outlines. They were always endowed with a non-laminated amorphous pith that was seen to vary in colour from the periphery to the inner part from

blue to light blue to colourless with Masson (Figure 7(A-B)) and Azan-Mallory trichrome (not shown). The inner pith appeared light blue-turquoise on staining with Alcian blue (not shown).

Nodular tracts of primary fibres. As revealed by SEM, the fibrous nodular tracts along the primary fibres frequently appeared almost hollow (Figure 5(A-B)). In LM sections, these nodular tracts had a pith containing resting and active zones of growing fibres, mature fibres, and filaments embedded in an amorphous material surrounded by a well-defined laminated outer bark characterized by clearly disjointed stratification (Figure 7(C-D)).

Proto-fibres originating ex novo. Fibres originating *ex novo* (187 to 433 μm in diameter) were seen to be
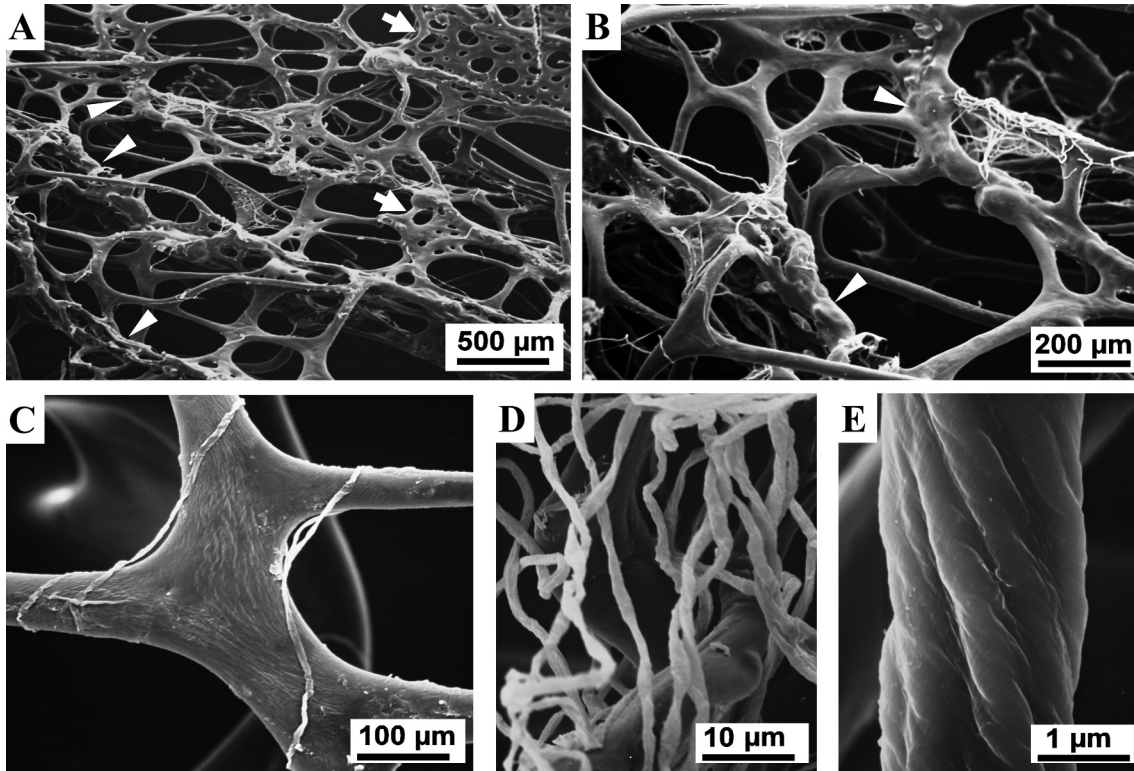
Figure 5. *Sarcotragus spinosulus*. SEM photo-micrographs of fibrous and filamentous skeletal network. (A). Main ascending, more or less parallel, primary fibres with linear tracts, nodular tracts (arrowheads), and cribrose plates (arrows) joining with thinner secondary fibres (see Figure 2 C, 7 A-B). (B). Nodular tracts (arrowheads) of primary fibres joining with trabecular cribrose plates and thinner secondary fibres (see Figure 6–7). Single, white filaments deriving from dissolved filamentous bundles are also present. (C). Fibres joined by fibrous cribrose plates. Single filaments deriving from dissolved filamentous bundles are also visible. (D-E). Filaments (dissociated) with surface highlighting wrapping and substructural architecture.

made up of a well-defined laminated outer bark with clearly disjointed stratification surrounding a central pith. The pith contained thick filaments (see below) embedded in an amorphous material and was characterized by the absence of cells (Figures 8–9). Filaments in the pith of the fibres were frequently associated with endobiotic microorganisms (see below) (Figure 8(B-D)). The thickness of the bark, which was composed of alternating layers (pink to light blue with Masson trichrome), varied considerably from a single very thin lamina (Figure 8(A-B)) up to multiple layers occupying more than the half of the diameter of the fibre (Figures 8(C-F), 9). In the proto-fibres with the thinnest bark, the outline of the bark was either wavy (Figure 8(A)) or more regular and circular (Figure 8(B)). Thickening of the bark was seen to occur through the inward deposition of multiple layers. Each pink layer of the growing bark was formed by a process of inward

apposition of pink granular structures within a light blue matrix, which were arranged in short parallel rows oriented perpendicularly to the inner surface of the bark (Figure 9(B)). During morphogenesis, the amorphous material in the pith of these structures appeared colourless or very light pink in the inner part and mainly colourless in the periphery on staining with Masson's trichrome, while it was light blue-turquoise with Alcian blue (Figure 9(C-D)). The amorphous material interposed between the layers was formed by the deposition of light blue filamentous-like material (Figure 9(B)).

Fibres inclusions. A few monaxial spicules and their fragments were embedded in the fibres, mainly parallel to the fibre axis; other particles of debris were also present (Figure 4).

In all the specimens examined, still unidentified, endobiotic microorganisms were strictly associated to
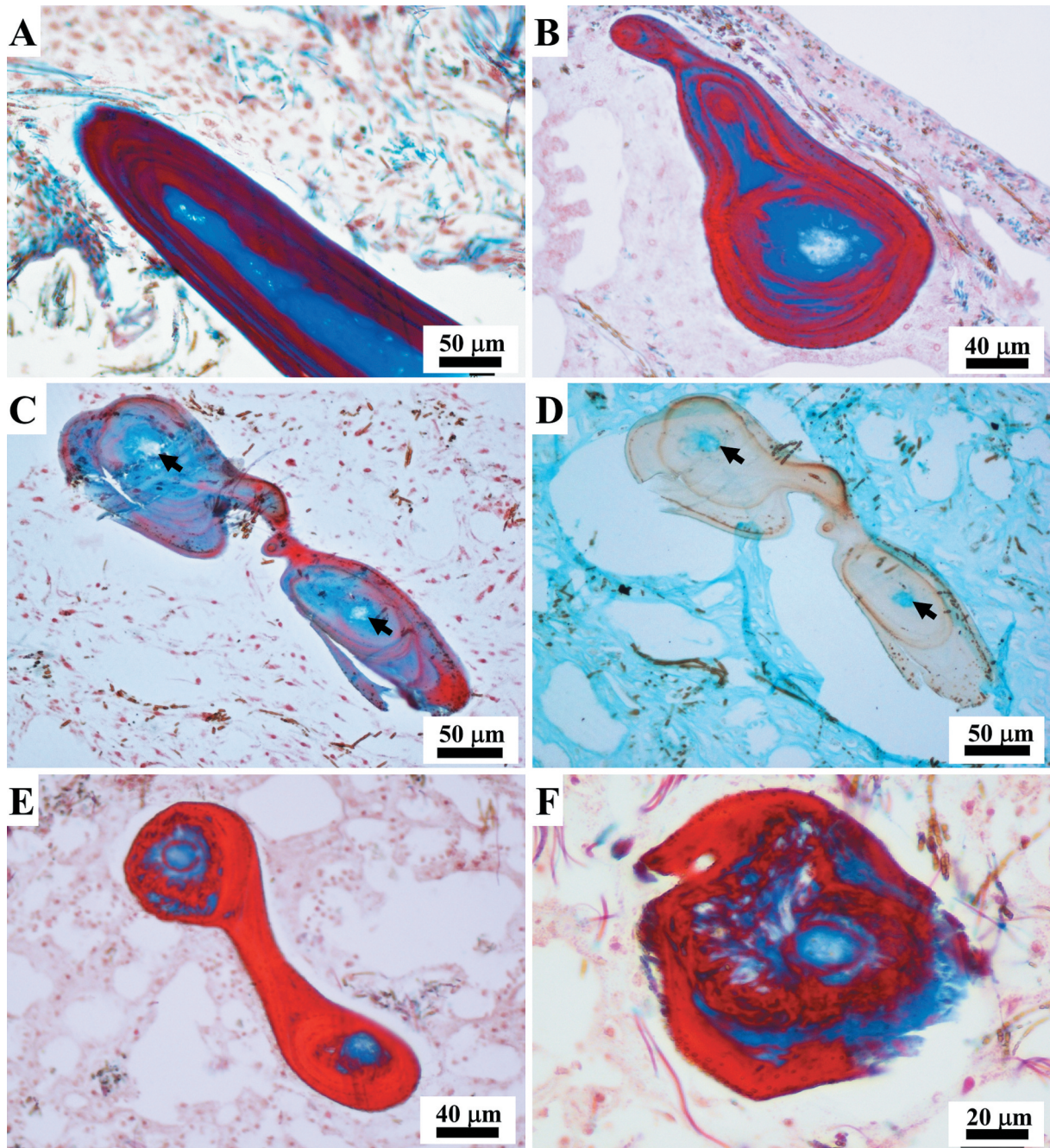
Figure 6. *Sarcotragus spinosulus*. LM photo-micrographs of skeletal histological sections. (A-C). Fibres with plurilamellar structure of bark (red) alternating with layers of amorphous matrix (blue) and amorphous non-laminated central core (light blue, blue-colourless) (arrows in C indicating the colourless inner core) (A, sagittal section; B, C, cross-section, Masson trichrome). (D). Fibres with a colourless laminated bark and turquoise innermost core (arrows) (cross-section, Alcian blue). (E-F). Fibres showing irregular scalloped outlines and a degenerating appearance of the bark (red) in the remodelling phase (cross-section, Masson trichrome). (C-D successive sections of the same fibre).
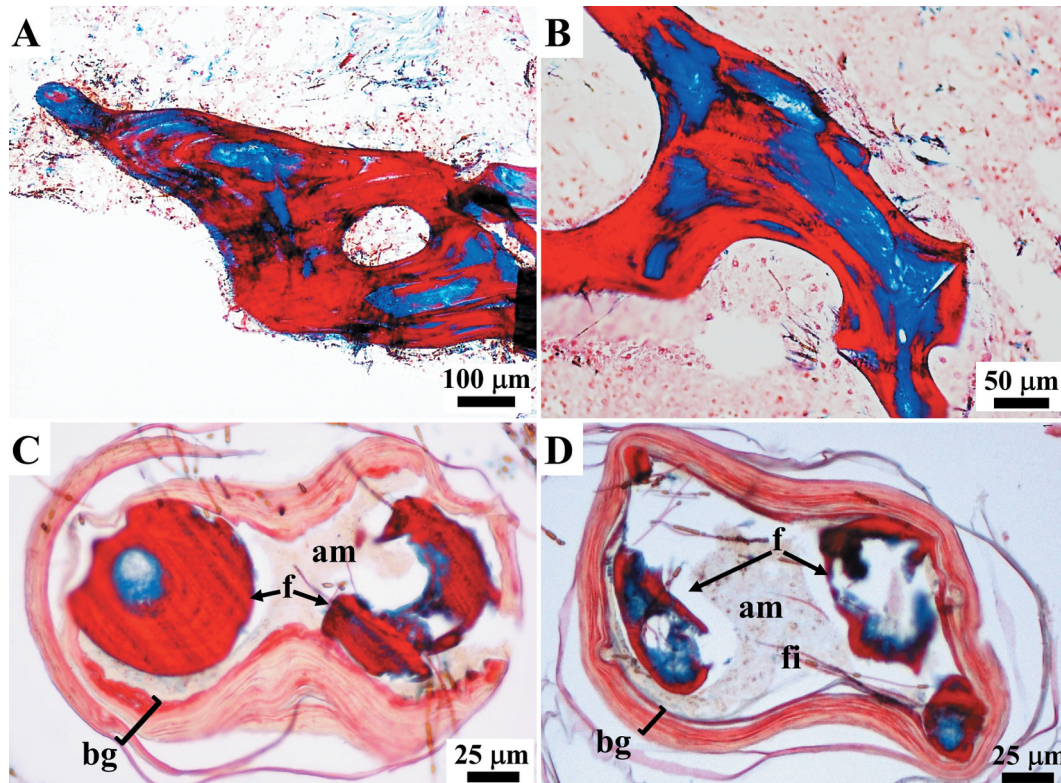
Figure 7. *Sarcotragus spinosulus*. LM photo-micrographs of skeletal histological sections. (A-B). Fibrous cribrose plates. (C-D). Fibrous nodular tracts showing remodelling fibres (F) embedded in amorphous material (am), and filaments (fi) surrounded by laminated growing bark (bg) (Masson trichrome). See also Figure 5(A-B).

the layers of the fibres (Figures 8(B, D), 10(E)). These associated microorganisms will be investigated in a companion paper.

Filamentous skeleton

The filamentous component occurred in the entire sponge body as thick filaments, mainly organized in bundles, and single thin filaments.

Thick filaments. Thick filaments (0.6–1.1 μm in diameter) were mainly organized in very abundant bundles, which were scattered singly or assembled in networks with various topographic and steric arrangements (Figures 2(C-D), 3(A-C), 4, 5, 7, 8, 9, 10(A-D), 11, 12(A, C-D)).

At the ectosomal level, a sub-dermal network (conular and interconular) oriented parallel to the body surface was composed by bundles of filaments variably oriented to form the net meshes (Figures 10(A-B), 11). In each conule variably oriented bundles of filaments supported the axial fibre (Figure 3(A-C)). In inner body regions, the bundles were scattered and variably oriented.

The filaments appeared blue on staining with Masson trichrome (Figure 10(A-D)) and Azan-Mallory trichrome (not shown). On confocal microscopy, the subdermal filamentous network was evident, and the filaments showed auto-fluorescence with a less fluorescent inner axis (Figure 11(B-C)).

Filamentous endobiotic microorganisms, still unidentified, were ubiquitous and strictly associated to the filaments (Figures 8–10).

Thin filaments. Scattered, rare single thin filaments (0.2–0.4 μm in diameter) characterized by terminal bulbar knobs were dispersed in the abundant ECM; bulbar knobs (2.6–4 μm in diameter) occur at the end of these filaments although in sections it is not possible to clearly define if knobs can occur at both or at a single end (Figures 4(B), 10(D-J)). In histological sections, these thin filaments showed a wavy course (Figure 10(D-J)) and appeared uniformly coloured, except for the terminal knobs. These latter were drop-shaped, and were all endowed with a rounded lighter core surrounded by a thin, more intensely coloured, layer (Figure 10(D-J)). In some cases, a structure made up of concentric layers was seen within the knobs (Figure 10(F, J)). On staining with
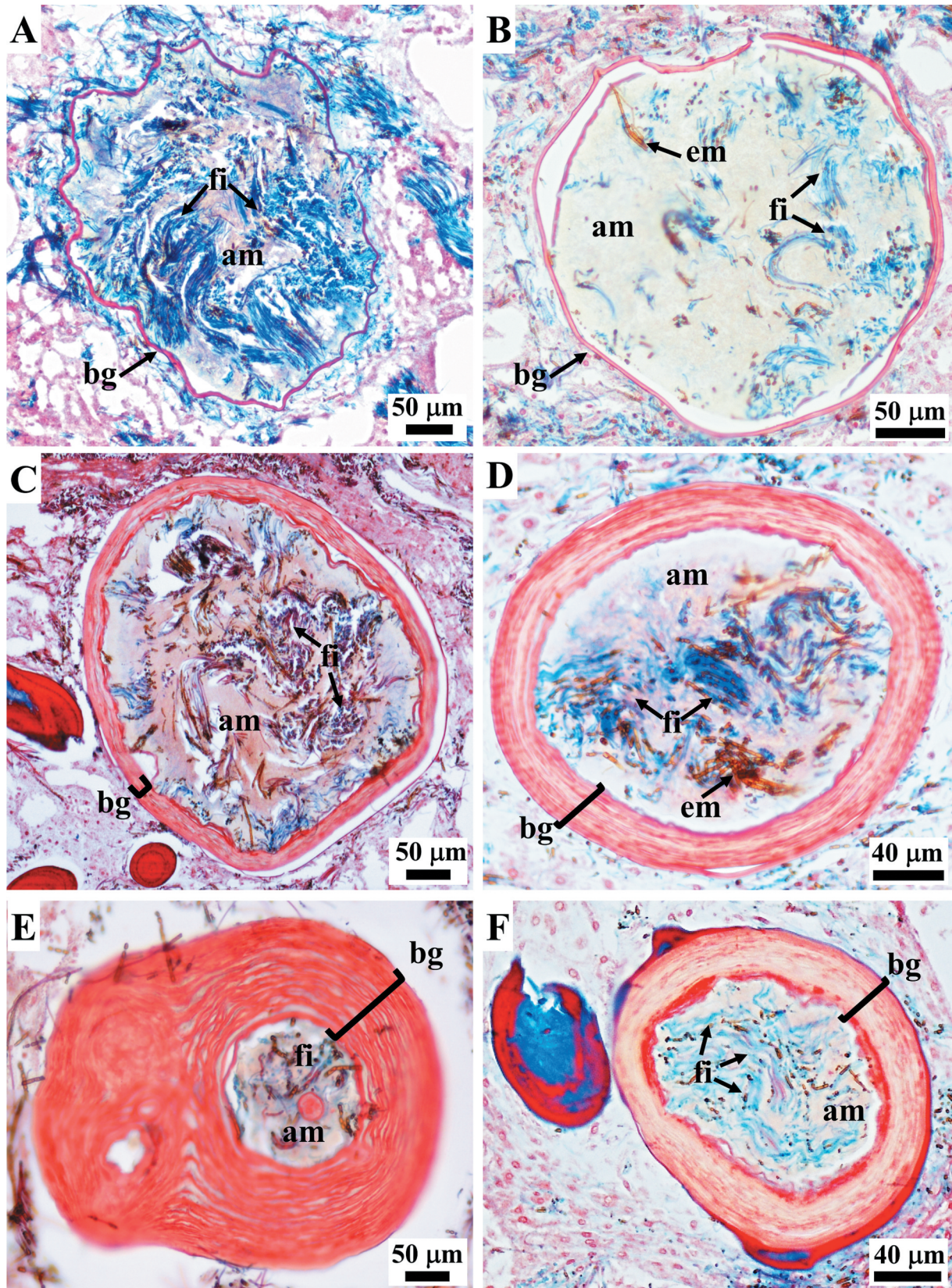
Figure 8. *Sarcotragus spinosulus*. LM photo-micrographs of skeletal histological sections. (A-E). Fibres showing laminated growing bark (salmon pink; bg) and a pith with filament bundles and single filaments (blue; fi) embedded in an amorphous material (pale yellowish; am). Associated endobiotic microorganisms (em) well evident in B-D. Note the progressive bark thickening and the reduction of the pith and the total fibre diameter. (F). Note the beginning of the bark maturation process starting from the outermost (red-blue) and thus oldest, layer. (Masson trichrome).
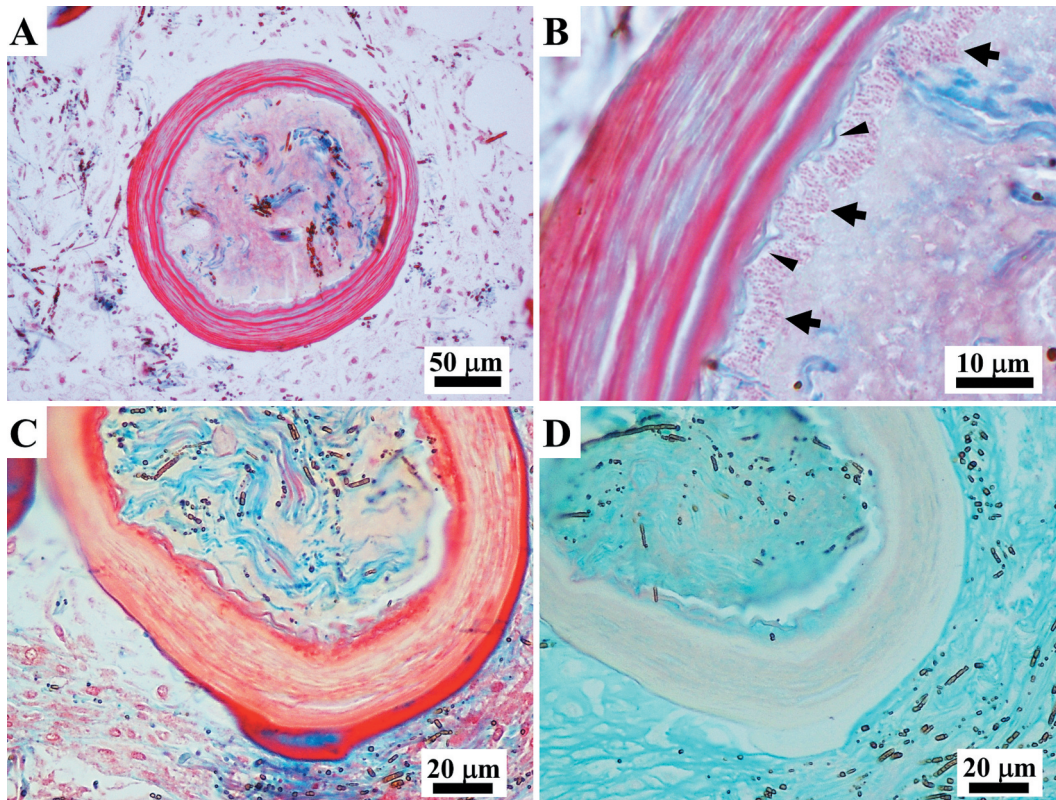
Figure 9. *Sarcotragus spinosulus*. LM photo-micrographs of skeletal histological sections. (A-B). Fibres showing the inner apposition of ordered laminae in the bark (pink) (arrows) and amorphous collagen material (light blue) (arrowheads) interposed between the layers. (C). Fibre with a pink laminated bark with the red, most external, layer and a core containing filaments (blue) embedded in an amorphous material (pale yellowish) (A-C cross-section, Masson trichrome). (D). Fibre with a colourless laminated bark and a core containing colourless filaments embedded in a turquoise amorphous glycosaminoglycan(GAG)-like material. Note the abundant GAG-like material also in the extracellular matrix (ECM) (cross-section, Alcian blue) (C-D successive sections of the same fibre).

Masson and Azan-Mallory trichrome these filaments appeared blue (Azan-Mallory not shown).

Collagen fibrils

Masson and Azan-Mallory trichrome revealed fibrillar collagen dispersed throughout the abundant ECM, mainly at the level of the ectosome appearing as fine light blue homogeneous material (Figure 12(A, C)), and in the regions surrounding aquiferous canals appearing as a pale blue trabecular network (Figure 12 (B, D)).

Discussion

Porifera evolved the ability to produce prototypes of the ECM and connective structures as organic skeletal system. The evolutionary novelty of exclusively collagenic skeletal structures components is an autapomorphy shared by Keratosa taxa. An autapomorphy exclusive of the family Irciniidae (order Dictyoceratida) is the filamentous skeleton associated to the fibrous one (Minchin 1900; Vacelet 1959; Garrone et al. 1973; Junqua et al. 1974; Cook & Bergquist 2002; Erpenbeck et al. 2020). It is known that *Sarcotragus spinosulus* is characterized by an irregularly reticulate spongin network of primary fibres lacking inclusions or bearing only rare foreign spicules, connected by secondary fibres and, as all Irciniidae, also by peculiar very thin knobended filaments together with fibrillar collagen dispersed throughout the ECM (Garrone et al. 1973; Bergquist 1978; Simpson 1984; Cook & Bergquist 2002; Gaino 2011; Pronzato & Manconi 2011; Manconi et al. 2013).

However, in our samples, we found some remarkable differences from the above-mentioned previous literature, and peculiarities of skeleton components, at the level of both composition and structure, that have never been reported before.
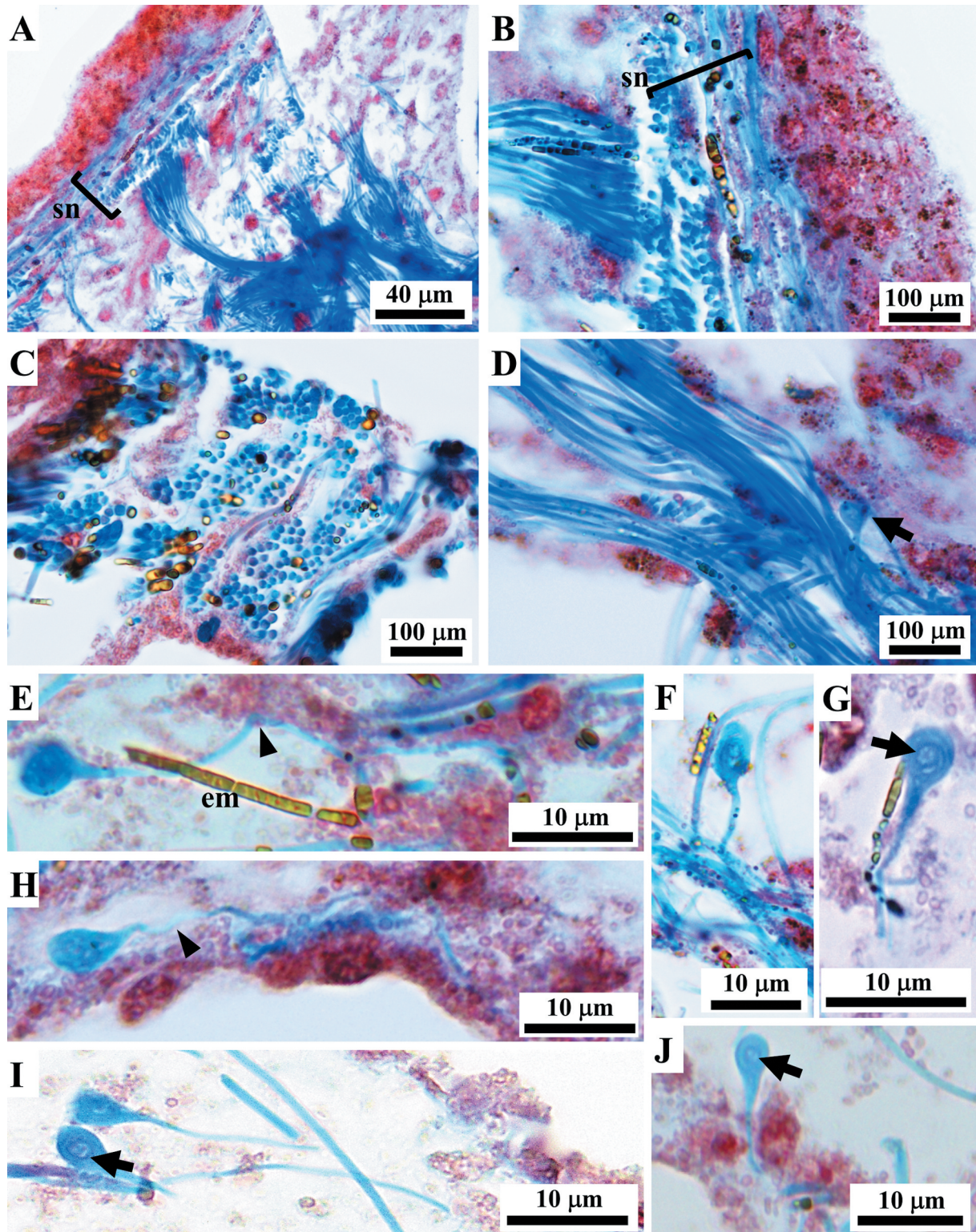
Figure 10. *Sarcotragus spinosulus*. LM photo-micrographs of skeletal histological sections. Associated endobiotic microorganisms (em) also evident. (A-B). Bundles of thick filaments with various orientations in the tangential subdermal network (sn; see Figure 11). (C). Bundles of thick filaments uniformly oriented (ectosome, cross-section). (D). Bundles of thick filaments and a single, thin knob-ended filament (arrow) (sagittal section). (E-J). Knob-ended thin filaments with wavy course (arrowheads) and drop-shaped knobs with evident lamellar structure surrounding a core (arrows). (Masson trichrome).
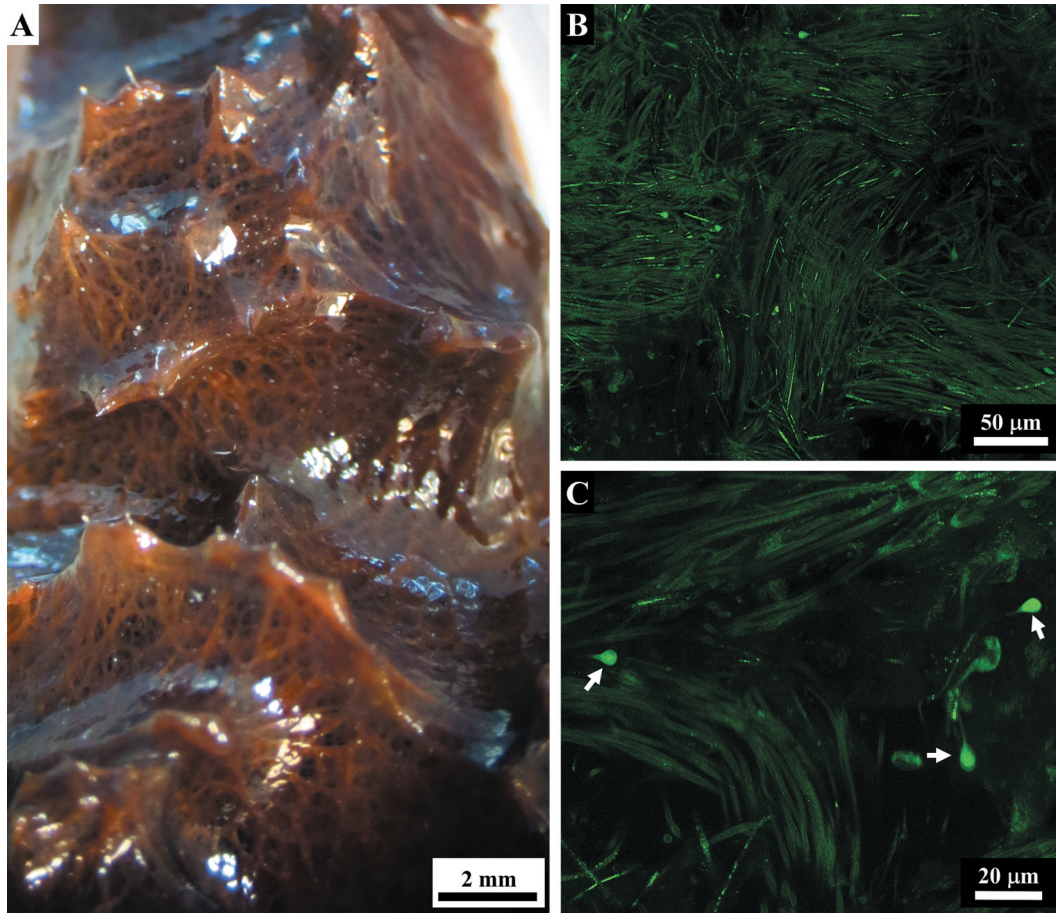
Figure 11. *Sarcotragus spinosulus*. Macro- and micro-photographs of subdermal filamentous skeleton. (A). Filamentous network supporting conules of a live sponge. (B). Bundles of filaments in the subdermal network (confocal microscope). (C). Rare knob-ended thin filaments (arrows) in the subdermal network of filament bundles (confocal microscope).

Fibres

Each mature primary fibre displays irregularly alternating linear, nodular, and laminar tracts along its length, all of which share in the bark concentric laminar growth lines alternating with layers of amorphous matrix. The fact that the inner pith appears colourless on staining with Masson and Azan-Mallory trichrome, and turquoise on staining with Alcian blue, indicates the presence of GAG-like molecules in this region. While the amorphous matrix of the fibres could be considered to have the same collagen composition as the thick filaments and knob-ended filaments (Figures 3, 6, 9), the laminar layers of fibres could correspond to peculiar morphs of collagen, i.e. spongin, which is exclusive to Porifera (Figures 3, 6). However, studies are in progress to clarify the nature of these different fibre components and, especially, to determine whether other macromolecules besides collagen are involved in fibre formation.

According to many authors, primary fibres in *S. spinosulus* are equipped with a "fibrillar" pith sensu Vacelet (1959), while secondary fibres are unpithed (Vacelet 1959; Boury-Esnault 1971; Cook & Bergquist 2002; Pronzato & Manconi 2011; Mercurio et al. 2013).

Interestingly, we found that mature primary and secondary fibres, regardless of their dimensions, together with cribrose plates, are always equipped with a non-laminated amorphous axial pith, and appear to be made up of collagen and, in the inner part, of GAG-like material. We may consider the "fibrillar-like" pith to be the pith that bears filaments in sections of newly formed and growing fibres (Figures 8–9).

Glycosaminoglycan-like were also observed in the ECM (Figures 6(D), 9(D)). The presence of GAG-like molecules has previously been reported in several species of horny sponges (see Formato et al. 2008; Langasco et al. 2017; and references therein). In a preliminary histological
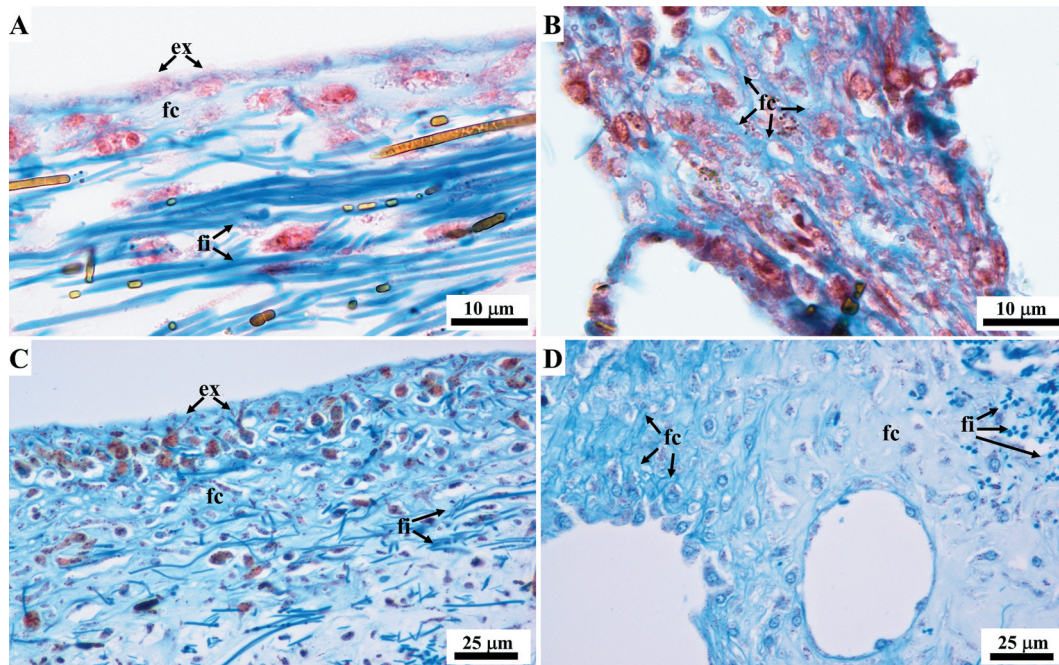
Figure 12. *Sarcotragus spinosulus*. LM photo-micrographs of histological sections showing the ECM collagen. (A, C). Ectosome, fibrillar collagen (fc) visible as a light blue fine homogeneous material. (B, D). ECM surrounding the aquiferous canals, fibrillar collagen (fc) visible as a light blue trabecular network. A-B Masson trichrome. C-D Azan-Mallory trichrome.

study, Manconi et al. (2002), (2006) observed these macromolecules also in the fibres of *S. spinosulus*.

The nodular tracts of primary fibres bearing resting and active zones of growth (Figure 7(C-D)) appear as morphogenetic regions in which the first stages of the growth process occur in the same way as that of the bark formation of newly formed fibres from which fibre growth and remodelling processes can start *ex novo* (see below).

Sequential phases of growth or remodelling processes occur in the fibres that originate *ex novo*, as is indicated by the fact that the larger the diameter of the fibres is, the smaller the thickness of its bark (blue) is, owing to compaction of the collagen structure. We found that, as the bark thickness of the fibres increases, the total diameter of the fibres decreases (Figures 8–9).

During fibres morphogenesis it can be hypothesized the following sequence of growth stages: (1) a very thin layer of bark bordering appears in an area of ECM rich in filaments and lacking cells; (2) the bark progressively thickens through the deposition of multiple alternate layers of proto-spongin and non-laminated collagen. This structural shift could be due to chemical and structural modification of the amorphous matrix/filaments and the resulting reduction of the central area of the fibre, which can be considered an axial pith; (3) further biochemical maturation and remodelling of the

proto-spongin layers occurs as the pith is filled with amorphous collagen material and GAG-like material (Figures 8, 9).

Thus, in *S. spinosulus*, the structure of the fibres seems to reach, during morphogenesis, its complex layout without the direct involvement of specialized cells driving the process, but means of modifications and new spatial assembly of pre-existing simpler collagen structures. This process occurs inwardly (i.e. the fibres grow by means of the inward deposition of successive layers) (Figure 9(B)); this is in contrast with the literature, according to which horny sponge fibres are synthesized by discrete groups of specialized cells driving also their assembling. In this regard, it has been reported that spongoblasts, by means of a "cooperative behaviour", first secrete the innermost part of the fibres, and then elongate and slide slowly down the fibre, laying down bark as they move (Vacelet 1971; Bergquist 1978; Simpson 1984; Gaino 2011). Thus, according to this latter hypothesis, bark construction occurs from the inside to the outside of the fibre, as shown by Vacelet (1971, Figure 1) in the case of *Aplysina aerophoba* (reported as *Verongia*). However, it has recently been demonstrated that *Aplysina* (Verongiida) has a skeleton composed in part by chitin (Klinger et al. 2014, 2019a, 2019b) with a composition diverging from that of *Sarcotragus* (Irciniidae, Keratosa), which is made of collagen. Moreover, according to recent molecular

analyses, the Verongomorpha and Keratosa subclasses diverge widely (Erpenbeck et al. 2012). It does not seem incongruous that different processes occur between distant taxa in the production of the skeleton.

Other morphogenetic processes, involving the degeneration and resorption of fibres, seem to lead to the remodelling of fibres (Figure 6(E-F)). These processes, together with those of the newly formed fibres and nodular tracts, may be related to the chronic morphogenesis and phenotypic plasticity typical of Porifera (see Gaino et al. 1995).

Filaments

The homogeneous collagen structure of filaments is confirmed by blue staining (Masson and Azan Mallory trichrome) although the terminal knobs bear a core that is sometimes surrounded by concentric lines.

By contrast, on confocal microscopy, the thick filaments appear less homogeneous, showing a less fluorescent internal axis. Using transmission electronic microscopy, Garrone et al. (1973) found that these filaments were made up of three layers: a cuticle-like outermost layer, a soft cylinder, and an axial central thread. Moreover, each filament appeared as bundles of microfibrils twisted in a helical fashion, nearly straight in the axis of the filament and becoming increasingly coiled toward the periphery, while the knob-ends corresponded to a denser, more disordered, spiralized region. Furthermore, Garrone et al. (1973) found that, in *S. spinosulus*, filaments organized in bundles were separated from one another by collagen trabeculae, which formed a sort of chamber around each filament. However, at the ectosomal level we found that filament bundles formed a more complex spatial structure as a sub-dermal network (Figures 3(A-C), 10(A-B), 11) and in each conule variably oriented bundles of filaments supported the axial fibre (Figure 3(A-C)). In other body regions, the bundles were scattered and variably oriented.

Several authors (Brien et al. 1973; Garrone et al. 1973; Gaino 2011) have claimed that the nature of filaments in the genera *Ircinia* and *Sarcotragus* is very similar to that of the spongin fibres. However, Junqua et al. (1974) reported that, in the genus *Ircinia* (formerly including the present *Sarcotragus*), fibres and filaments differed in terms of their chemical composition, behaviour in alkali and morphology, suggesting that they may have different mechanisms of biosynthesis and organization. Similarly, our results demonstrated that, in *S. spinosulus*, the filaments showed a different composition and structure from that of the fibres.

Interestingly, we found that, in *S. spinosulus*, the number of terminal knobs was much lower than that of the filaments. Knobs were localized at the terminal end of very thin filaments, which were mainly seen scattered in the ECM and were not associated with the typical filament bundles of this species. Moreover, as we never found filaments with two knobs, the occurrence of knobs at both terminal ends in *S. spinosulus* was not confirmed. Further comparative studies are in progress with the aim of shedding light on these skeleton components.

Fibrillar collagen

Collagen occurring as fibrils is usually dispersed throughout the ECM, and its organization needs electron microscopy investigation (Garrone et al. 1973; Gaino 2011; Ehrlich et al. 2018). However, this component of the ECM can also be revealed by means of some histological stains. Gross et al. (1956) called this collagen material (fine blue staining with Mallory aniline blue or Masson trichrome) "spongin A" and noted that it was distributed throughout the body as a ramifying reticular meshwork of the horny sponge *Spongia graminea* Hyatt, 1877 (currently *Spongia (Spongia) graminea*). Similarly, in our study, ECM fibrillar collagen was highlighted as a trabecular network (Figure 12(B, D)), presumably corresponding to the so-called "chondrochyma" reported in other species by some authors (see Minchin 1900; Cowden & Harrison 1976), and also as fine amorphous material (Figure 12(A, C, D)), but mainly at the level of the ectosome and the regions surrounding canals of the aquiferous system.

Morphofunctional aspects

The morphofunctional role of skeletal collagen networks as a supporting structure clarifies some aspects of the evolution of ECM prototypes in the background of the huge morphofunctional plasticity displayed by Porifera.

Indeed, our data on *Sarcotragus spinosulus* indicate a supportive functional role (a) of the tangential sub-dermal filamentous network, and fibrillar collagen, at the sponge surface, which maintain the dermal membrane; (b) of the variably oriented bundles of filaments in conular areas cooperating with distal portions of the fibres that act as the conular axis; (c) of fibrillar collagen and associated GAGs-like molecules acting as layout to balance water retention in the jelly-like ECM and to water pumping and circulation during the contraction/relaxation phases of the areas surrounding the aquiferous system. The

topographic distribution of all these skeletal collagen elements is fundamental to the body plan of the sponge and its physiological performance.

Conclusions

The auto-assembling and remodelling processes occurring in fibres morphogenesis from collagenic structures preexisting in the ECM, as found out in our experimental model, seem to be an evolutionary novelty for the genus *Sarcotragus* and, more in general, for basal Metazoa. Our results indicate that knowledge on morphogenesis, morpho-anatomical and functional architecture of sponges could be a key tool in the field of applied research for identifying and defining the potentialities of biomaterials in organisms provided with a skeleton rich in collagen. Last but not least, this kind of dataset could contribute to clarify the problematic status of the family Irciniidae from a systematic and phylogenetic point of view.

Disclosure statement

The authors declare no competing interests.

ORCID

G. A. Stocchino http://orcid.org/0000-0002-7005-208X
T. Cubeddu http://orcid.org/0000-0001-7522-8200
R. Pronzato http://orcid.org/0000-0003-1355-0936
M. A. Sanna http://orcid.org/0000-0001-7941-2355
R. Manconi http://orcid.org/0000-0002-7619-8493

References

Bergquist PR. 1978. Sponges. Los Angeles (USA): Hutchinson University Library, London & University of California Press.

Bergquist PR, Walsh D, Gray RD. 1998. Relationships within and between the orders of Demospongiae that lack a mineral skeleton. In: Watanabe Y, editor. Sponge science: Multidisciplinary perspectives. Tokyo: Springer. pp. 31–40.

Boury-Esnault N. 1971. Spongiaires de la zone rocheuse littorale de Banyuls sur Mer. II. Systématique. Vie et Milieu 22 (2):287–349.

Brien P, Lévi C, Sarà M, Tuzet O, Vacelet J. 1973. Spongiaires. In: Grassé PP, editor. Traité de Zoologie. Anatomie, Systématique, Biologie. Spongiaires. Paris: Masson et C.ie Editeurs Vol. 3(l), pp. 716.

Cook S de C, Bergquist PR. 2002. Order Dictyoceratida Minchin, 1900. In: Hooper JNA, van Soest RWM, editors. Systema Porifera: A guide to the classification of sponge. New York: Kluwer Academic/Plenum Publishers. pp. 1021–1066. DOI: 10.1007/978-1-4615-0747-5_98.

Cowden RR. 1970. Connective tissue in six marine sponges: A histological and histochemical study. Zeitschrift fur mikroskopisch-anatomische Forschung 82(4):557–569.

Cowden RR, Harrison FW. 1976. Cytochemical studies of connective tissues in sponges. In: Harrison FW, Cowden RR, editors. Aspects of sponge biology. New York: Academic Press. pp. 69–82. DOI: 10.1016/B978-0-12-327950-7.50011-7.

Ehrlich H, Wysokowski M, Zoltowska-Aksamitowska S, Petrenko I, Jesionowski T. 2018. Collagens of poriferan origin. Marine Drugs 16:79. DOI: 10.3390/md16030079.

Erpenbeck D, Galitz A, Ekins M, Cook S de C, van Soest RW, Hooper JN, Wörheide G. 2020. Soft sponges with tricky tree: On the phylogeny of dictyoceratid sponges. Journal of Zoological Systematics and Evolutionary Research 58 (1):27–40. DOI: 10.1111/jzs.12351.

Erpenbeck D, Sutcliffe P, Cook S de C, Dietzel A, Maldonado M, Van Soest RWM, Hooper JNA, Wörheide G. 2012. Horny sponges and their affairs: On the phylogenetic relationships of keratose sponges. Molecular Phylogenetics and Evolution 63(3):809–816. DOI: 10.1016/j.ympev.2012.02.024.

Formato M, Lepedda AJ, Ledda FD, Cigliano A, Zinellu E, Pronzato R, Cherchi GM, Manconi R. 2008. Glycosaminoglycan diversity in marine sponge extracellular matrix. Proceedings of SardiniaChem2008, Sassari, Italy, pp. 76–77.

Gaino E. 2011. Overview of Porifera. In: Pansini M, Manconi R, Pronzato R, editors. Fauna d'Italia. Porifera I. Calcarea, Demospongiae (partim), Hexactinellida, Homoscleromorpha. Vol. 46. Bologna: Calderini-Il Sole 24 Ore. pp. 1–53.

Gaino E, Manconi R, Pronzato R. 1995. Organizational plasticity as a successful conservative tactics in sponges. Animal Biology 4:31–43.

Garrone R. 1978. Phylogenesis of connective tissue. Morphological aspects and biosynthesis of sponge intercellular matrix. Basel: S. Karger. pp. 252.

Garrone R. 1985. The collagen of the Porifera. In: Bairati A, Garrone R, editors. Biology of invertebrates and lower vertebrates collagens. New York: Plenum Press. pp. 157–182. DOI: 10.1007/978-1-4684-7636-1_12.

Garrone R, Vacelet J, Pavans de Ceccatty M, Junqua S, Robert L, Huc A. 1973. Une formation collagène particulière: les filaments des éponges cornées *Ircinia*. Étude ultrastructurale, physicochimique et biochimique. Journal de Microscopie 17:241–260.

Gross J, Sokal Z, Rougvie M. 1956. Structural and chemical studies on the connective tissue of marine sponges. Journal of Histochemistry & Cytochemistry 4(3):227–246. DOI: 10.1177/4.3.227.

Hooper JNA, van Soest RWM, editors. 2002. Systema Porifera: A guide to the classification of sponges. New York: Kluwer Academic/plenum Publishers. https://doi.org/10.1007/978-1-4615-0747-5.

Junqua S, Robert L, Garrone R, Pavans de Ceccatty M, Vacelet J. 1974. Biochemical and morphological studies on collagens of horny sponges. *Ircinia* filaments compared to spongines. Connective Tissue Research 2:193–203. https://doi.org/10.3109/03008207409152244.

Klinger C, Żółtowska-Aksamitowska S, Jesionowski T. 2019a. Isolation of chitin from *Aplysina aerophoba* using a microwave approach. Progress on Chemistry and Application of Chitin and Its Derivatives 24:61–74. DOI: 10.15259/PCACD.24.005.

Klinger C, Żółtowska-Aksamitowska S, Wysokowski M, Tsurkan MV, Galli R, Petrenko I, Machałowski T, Ereskovsky A, Martinović R, Muzychka L, Smolii OB, Bechmann N, Ivanenko V, Schupp PJ, Jesionowski T, Giovine M, Joseph Y, Bornstein SR, Voronkina A, Ehrlich H. 2019b. Express method for isolation of ready-to-use 3D Chitin Scaffolds from *Aplysina archeri* (Aplysineidae: Verongiida) Demosponge. Marine Drugs 17(2):131. DOI: 10.3390/md17020131.

Klinger CS, Machill S, Niemann H, Proksch P, Brunner E. 2014. The skeletal amino acid composition of the marine demosponge *Aplysina cavernicola*. Marine Drugs 12(8):4417–4438. DOI: 10.3390/md12084417.

Langasco R, Cadeddu B, Formato M, Lepedda AJ, Cossu M, Giunchedi P, Pronzato R, Rassu G, Manconi R, Gavini E. 2017. Natural collagenic skeleton of marine sponges in pharmaceutics: Innovative biomaterial for topical drug delivery. Materials Science and Engineering C, 70:710–720.

Manconi R, Cadeddu B, Ledda FD, Pronzato R. 2013. An overview of the Mediterranean cave-dwelling horny sponges (Porifera, Demospongiae). ZooKeys 28:1–68. DOI: 10.3897/zookeys.281.4171.

Manconi R, Corso G, Formato M, Stocchino GA, Pronzato R. 2002. Morfogenesi cronica dei poriferi: la strutturazione della matrice extracellulare è modulata dai glicosaminoglicani? 63° Convegno Unione Zoologica Italiana, Rende, Italy.

Manconi R, Ortu MF, Ledda FD, Stocchino GA, Corso G. 2006. Skeletal fibers of *Sarcotragus spinosulus* and *Aplysina aerophoba* (Porifera, Demospongiae): A histochemical study during regeneration. 7th International Sponge Symposium, Brazil.

Manconi R, Padiglia A, Cubeddu T, Pronzato R. 2020. Long-term sponge stranding along the shores of Sardinia Island (Western Mediterranean Sea). Marine Ecology 40(6): e12567. DOI: 10.1111/maec.12567.

Manconi R, Padiglia A, Padedda BM, Pronzato R. 2020. Invasive green algae in a western Mediterranean Marine Protected Area: Interaction of photophilous sponges with *Caulerpa cylindracea*. Journal of the Marine Biological Association of the United Kingdom 100:361–373. DOI: 10.1017/S0025315420000193.

Mercurio M, Corriero G, Gherardi M, Baldacconi R, Gaino E. 2013. Sexual reproduction in *Sarcotragus spinosulus* from two different shallow environments. Marine Ecology 34:394–408. DOI: 10.1111/maec.12039.

Minchin EA. 1900. Chapter III. Sponges. In: Lankester EBR, editor. A treatise on zoology. Part II. The Porifera and Coelenterata. London: Adam & Charles Black. pp. 1–178.

Padiglia A, Ledda FD, Padedda BM, Pronzato R, Manconi R. 2018. Long-term experimental in situ farming of *Crambe crambe* (Demospongiae: Poecilosclerida). PeerJ 6:e4964. DOI: 10.7717/peerj.4964.

Perez-Lopez P, Ledda FD, Bisio A, Feijoo G, Perino E, Pronzato R, Manconi R, Moreira MT. 2017. Life cycle assessment of in situ mariculture in the Mediterranean Sea for the production of bioactive compounds from the sponge *Sarcotragus spinosulus*. Journal of Cleaner Production 142:4356–4368. DOI: 10.1016/j.jclepro.2016.11.137.

Pronzato R, Manconi R. 2011. Class Demospongiae. Orders Dendroceratida, Dictyoceratida, Verongida, Halisarcida. In: Pansini M, Manconi R, Pronzato R, editors. Fauna d'Italia. Porifera I. Calcarea, Demospongiae (partim), Hexactinellida, Homoscleromorpha. Vol. 46. Bologna: Calderini-Il Sole 24 Ore. pp. 245–340.

Simpson TL. 1984. The cell biology of sponges. New York: Springer-Verlag. https://doi.org/10.1007/978-1-4612-5214-6.

Vacelet J. 1959. Repartition generale des eponges et systematique des epongés cornées de la region de Marseille et de quelques stations mediterraneennes. Recueil des Travaux de la Station Marine d'Endoume 16:39–101.

Vacelet J. 1971. Ultrastructure et formation des fibres de spongine d'Eponges Cornees *Verongia*. Journal de Microscopie 10:13–32.